◆ Human Brain Mapping 37:2210–2222 (2016) ◆

Structural Connectivity of the Human Anterior Temporal Lobe: A Diffusion Magnetic Resonance Imaging Study

Nico Papinutto,[1]* Sebastiano Galantucci,[2] Maria Luisa Mandelli,[1] Benno Gesierich,[3] Jorge Jovicich,[4] Eduardo Caverzasi,[1] Roland G. Henry,[1] William W. Seeley,[1] Bruce L. Miller,[1] Kevin A. Shapiro,[1] and Maria Luisa Gorno-Tempini[1]

[1]*Department of Neurology, University of California San Francisco, San Francisco, CA, USA*
[2]*Neuroimaging Research Unit, Institute of Experimental Neurology, Division of Neuroscience, San Raffaele Scientific Institute, Vita-Salute San Raffaele University, Milan, Italy*
[3]*Institute for Stroke and Dementia Research, Ludwig-Maximilians-University, Munich, Germany*
[4]*Center for Mind/Brain Sciences (CIMEC), University of Trento, Rovereto, Italy*

Abstract: The anterior temporal lobes (ATL) have been implicated in a range of cognitive functions including auditory and visual perception, language, semantic knowledge, and social-emotional processing. However, the anatomical relationships between the ATLs and the broader cortical networks that subserve these functions have not been fully elucidated. Using diffusion tensor imaging (DTI) and probabilistic tractography, we tested the hypothesis that functional segregation of information in the ATLs is reflected by distinct patterns of structural connectivity to regions outside the ATLs. We performed a parcellation of the ATLs bilaterally based on the degree of connectivity of each voxel with eight ipsilateral target regions known to be involved in various cognitive networks. Six discrete segments within each ATL showed preferential connectivity to one of the ipsilateral target regions, via four major fiber tracts (uncinate, inferior longitudinal, middle longitudinal, and arcuate fasciculi). Two noteworthy interhemispheric differences were observed: connections between the ATL and orbito-frontal areas were stronger in the right hemisphere, while the consistency of the connection between the ATL and the inferior frontal gyrus through the arcuate fasciculus was greater in the left hemisphere. Our findings support the hypothesis that distinct regions within the ATLs have anatomical connections to different cognitive networks. *Hum Brain Mapp 37:2210–2222, 2016*.

Key words: anterior temporal lobe; diffusion tensor imaging; healthy subjects; parcellation; structural connectivity

INTRODUCTION

Over the past several decades it has become increasingly evident that the anterior temporal lobes (ATLs) play a crucial role in the representation of semantic knowledge. Perhaps the most widely accepted hypothesis is that the ATL serves as a "semantic hub"—a modality- and category-general association area that links anatomically distributed knowledge about various semantic features of concepts

*Correspondence to: Nico Papinutto, PhD; Department of Neurology, University of California, San Francisco, CA, USA. E-mail: nico.papinutto@ucsf.edu

Received for publication 15 September 2015; Revised 10 February 2016; Accepted 21 February 2016.

DOI: 10.1002/hbm.23167

Published online 4 March 2016 in Wiley Online Library (wileyonlinelibrary.com).

(shape, action, color, typical location, etc.), together with concept names, regardless of the task that is to be performed (e.g., naming an object, drawing it, or using it) [Patterson et al., 2007]. This view draws considerable support from studies of patients with the semantic variant of primary progressive aphasia (svPPA) [Bozeat et al., 2000], which is associated (at least in its early stages) with focal degeneration of the anterior temporal lobes, maximal at the poles, and adjacent rostral-inferior regions [Gorno-Tempini et al., 2004].

Taken at face value, the semantic hub model predicts that damage to the anterior temporal lobes should result in difficulty accessing conceptual knowledge independent of the modality of input or output, and independent of semantic category. This is broadly true for patients with svPPA, and is congruent with neuroimaging findings that the anterior temporal lobes are structurally and functionally connected to a distributed network of modality-selective and transmodal cortical regions [Guo et al., 2013; Pascual et al., 2015], including classical language regions [Binney et al., 2012]. Similarly, in support of this assumption, it has been shown that transcranial magnetic stimulation of the anterior temporal lobe results in category-general slowing of naming, while category-specific effects can be obtained by stimulation of the inferior parietal lobe [Pobric et al., 2009, 2010a, 2010b].

Functional Dissociations Within the Anterior Temporal Lobes

On the other hand, studies of patients with impairments in semantic processing due to a wide range of pathological processes—including stroke, neurodegenerative disease, herpes simplex virus encephalitis, and surgical resection—have suggested an anatomical sensitivity to knowledge about different conceptual categories within the temporal lobes, with portions of the ATLs involved preferentially in processing information about certain kinds of concepts, such as living things, artifacts, and proper names [Bi et al., 2011; Brambati et al., 2006; Damasio et al., 2004; Noppeney et al., 2007]. Contrary to the view of the ATL as an undifferentiated semantic hub, these studies indicate that distinct regions within the ATL—perhaps organized in a medial-to-lateral fashion—might be involved in processing knowledge relevant to different conceptual domains. Moreover, the right and left ATL may contribute differentially to different aspects of semantic and social/appraisal processing. For example, the execution of empathic tasks and emotion processing seem to be more impaired by atrophy of the right ATL [Rankin et al., 2006; Seeley et al., 2005; Thompson et al., 2003], while it has been proposed that the left ATL is particularly important for retrieval of concept names [Schwartz et al., 2009]—though perhaps only in conjunction with a broader left-lateralized language network [Newhart et al., 2007; Tsapkini et al., 2011].

This problem is compounded by apparently conflicting evidence from functional neuroimaging studies. Although some studies using positron emission tomography have suggested that there is category selectivity within the ATL [Damasio et al., 1996, 2004; Devlin et al., 2002; Kellenbach et al., 2005; Moore and Price, 1999; Mummery et al., 1996], studies using functional magnetic resonance imaging (MRI) have largely shown category-selective activation in more posterior parts of the temporal lobe, including the middle temporal gyrus, superior temporal gyrus/sulcus, and fusiform gyri, as well as posterior parietal regions [Chao et al., 1999; Mahon and Caramazza, 2009; Mahon et al., 2007; Martin and Chao, 2001].

In part, this discrepancy may be due to technical difficulties in measuring the BOLD signal from the anterior temporal lobes [Binder et al., 2009; Devlin et al., 2000].

A few more recent studies using distortion-corrected fMRI methods have indeed shown that semantic decision across a wide variety of stimuli engages the ventral anterior temporal lobes, but that there are modality-specific differences across stimuli: pictures and environmental sounds produce bilateral activation, while auditory words produce more left-sided activation [Visser and Lambon Ralph, 2011]. Moreover, there appears to be a gradation in activation for information from different modalities within the ATLs, with verbal information eliciting more superior-medial regions and visual information activating infero-lateral regions [Visser et al., 2012]. This may reflect different strengths of connections between these portions of the ATL and modality-specific regions in the posterior temporal lobes and other parts of the brain.

Taken together, the data available from neuropsychological and functional imaging in healthy controls suggests not only that the ATL as a whole is connected to a more anatomically distributed semantic network [Guo et al., 2013; Patterson et al., 2007] but also that there may be regions within the ATL with preferential connectivity to specific posterior temporal, frontal, and parietal areas [Visser and Lambon Ralph, 2011; Visser et al., 2012], underlying the apparent category-selectivity of some ATL lesions [Guo et al., 2013; Pascual et al., 2015; Patterson et al., 2007].

Structural Parcellation of the Anterior Temporal Lobes

Histologic studies also support the idea that the ATL is composed of anatomically distinct subregions with potentially different patterns of long-range connectivity [Blaizot et al., 2010; Ding et al., 2009; Flechsig, 1920; Hopf, 1954]. For instance, Ding et al. [2009] used modern neuroanatomical techniques and a combination of cellular, neurochemical, and neuropathological markers to show that the temporal polar cortex (TPC) could be parcellated into seven different areas with different anatomical and biochemical profile. Tracer studies in the temporo-polar

cortex of primates similarly suggest that multiple streams of information converge in the ATL, with graded differences in connection strengths [Morán et al., 1987].

Finally, there is evidence for structural parcellation within the ATL from human *in vivo* studies using diffusion tensor imaging methods to distinguish ATL subregions based on patterns of long-range connectivity. For example, Binney et al. [2012] demonstrated differential connectivity of left hemisphere rostral, mid, and caudal temporal lobe regions with perisylvian regions known to be involved in language processing (in contrast to the pattern of intra-temporal connections, which showed robust interconnectivity between all regions in caudal-to-rostral and lateral gradients) [Binney et al., 2012]. Connectivity between the ATL and regions outside the classical language network was not studied.

More recently, Fan et al. [2014] used a combination of diffusion tensor imaging and functional connectivity techniques to distinguish three subregions within the temporal pole: a dorsal region connected to the superior temporal gyrus, orbital part of the inferior frontal cortex, and insular cortex; a lateral region connected to the orbital part of the superior frontal gyrus and areas associated with the so-called default mode network; and a medial part with connections to the ventral and lateral temporal lobes [Fan et al., 2014].

Here, we used diffusion tensor imaging techniques to specifically explore the connectivity of the right and left ATL to posterior temporal regions implicated in visual and auditory perception (superior temporal and occipital), semantic and language processing (temporal, inferior frontal, angular and supramarginal gyri), and emotion processing (orbitofrontal cortex). This is the first study to investigate the connectivity of the ATLs with homolateral regions of the brain outside the conventional language network. It builds upon previous work [Binney et al., 2012; Pascual et al., 2015] in particular by examining differential connectivity of the ATLs (beyond the temporal poles) in both the left and right hemispheres.

We hypothesize a differential lateral–ventral distribution of connections within ATL depending on connectivity to auditory, visual, and language processing areas, and a differential medial–lateral and hemispheric distribution in relation the more crucial role of the medial and right-sided ATL in social–emotional processing.

MATERIALS AND METHODS

Subjects

Twenty-one healthy subjects (mean age 65.3 ± 3.6 years, 8 males and 13 females), with no history of psychiatric, neurological, or cognitive impairment, were recruited at the Memory and Aging Center, University of California, San Francisco (UCSF). All participants gave written informed consent, and the study was approved by the UCSF Committee on Human Research. The healthy subjects were selected to match the age of patients in frontotemporal dementia studies and received a comprehensive evaluation including history and neurological examination, neuropsychological testing, and neuroimaging. Demographic and clinical data for the subjects included in the study are reported in Table I.

TABLE I. Demographic and clinical data (mean and standard deviation at the time the MRI scans were performed) of the subjects included in the study

	Subjects
Age (years)	65.3 (3.6)
Gender (M/F)	8/13
Education (years)	17.3 (2.3)
Handedness (L/R)	2/19
MMSE (30)	29.5 (0.7)

MMSE: Mini-Mental State Examination.

MRI Acquisition

MRI images were acquired on a 3 T Siemens Trio Tim scanner equipped with whole body transmit and eight-channel receive head coils. A standard 3D MPRAGE T1-weighted structural image was acquired with the following parameters: sagittal acquisition, 160 slices per slab, voxel size = 1 × 1 × 1 mm^3, matrix size = 256 × 240, repetition time (TR) = 2300 ms, echo time (TE) = 2.98 ms, inversion time (TI) = 900 ms, flip angle = 9°. In addition, a 3D FLAIR sequence was acquired to exclude the presence of significant vascular disease in the subjects. Sequence parameters were as follows: sagittal acquisition, 160 slices per slab, voxel size = 1 × 1 × 1 mm^3, matrix size = 256 × 258, TR/TE = 6000 ms/389 ms; TI = 2100 ms; flip angle = 120°.

Diffusion-weighted images (DWI) were acquired using a 2D single-shot spin-echo echo-planar sequence (2D SE-EPI), 55 contiguous axial slices, voxel size = 2.2 × 2.2 × 2.2 mm^3, matrix size = 100 × 100, TR/TE = 8000 ms/109 ms, flip angle = 90°, generalized autocalibrating partially parallel acquisition (GRAPPA) factor 2; number of acquisition (NEX) = 1. One image without any sensitizing diffusion gradient applied (hereafter called b0) was acquired together with 64 DWI with diffusion gradients (b = 2000 s/mm^2) applied along unique directions that were defined by an electrostatic repulsion algorithm.

MRI Data Preprocessing

Preprocessing of MRI datasets was performed using the FMRIB FSL library tools (http://www.fmrib.ox.ac.uk/fsl/) [Smith et al., 2004; Woolrich et al., 2009].

The T1-weighted data were skull stripped, removing all the nonbrain tissue, by using the Brain Extraction Tool

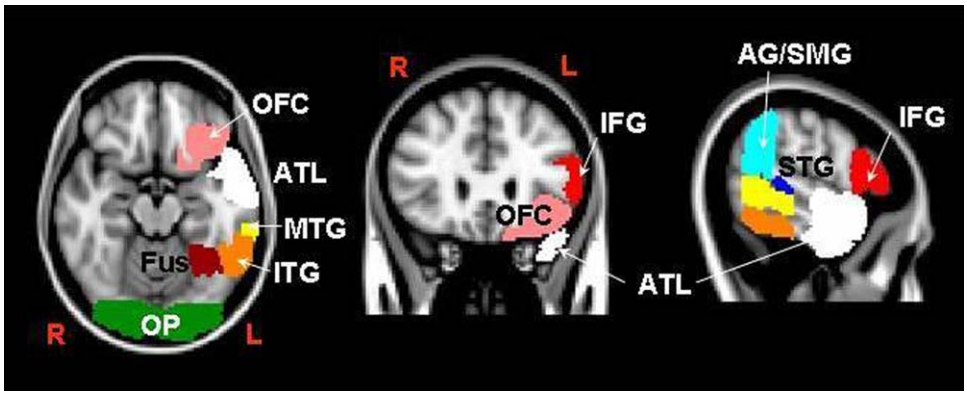

Figure 1.

Seed and target regions used for the parcellation of the left ATL and for the reconstruction of the tracks (symmetrical regions for the right hemisphere not reported): (1) anterior temporal lobe (ATL, white), (2) occipital pole (OP, green), (3) pars triangularis and pars opercularis of the inferior frontal gyrus (IFG, red), (4) orbitofrontal cortex (OFC, pink), (5) angular gyrus and posterior division of the supramarginal gyrus (AG/SMG, light blue), (6) temporo-occipital fusiform cortex (Fus, dark red), and posterior and temporo-occipital divisions of (7) the inferior temporal gyrus (ITG, orange), (8) the middle temporal gyrus (MTG, yellow), and (9) the superior temporal gyrus (STG, blue).

(BET) and they were subsequently aligned to MNI space using linear (FLIRT) and nonlinear transformations (FNIRT). All transformations were inverted and inverse transformation matrices and warp fields were obtained. BET results were visually inspected and, when needed, manual adjustments were performed to correct skull stripping errors.

The diffusion-weighted images were skull stripped and corrected for eddy current (EC) distortions and motion artifacts using affine registration to the b0 volume. All subjects' EC corrected data were visually checked to exclude possible errors in the affine registration process. Fractional anisotropy (FA), Mean Diffusivity (MD) and principal eigenvalue (λ_1, λ_2, λ_3) maps were obtained from the EC corrected, skull stripped diffusion data using the FDT diffusion tool. Each subject's FA map was transformed to the MNI space by means of linear and nonlinear transformations, using each subject's T1-weighted scan as an intermediate step. Finally, inverse transformation matrices of these FA to MNI transformations were computed.

Definition of ROIs

For the structural connectivity analysis, we defined one seed and eight target regions of interest (ROIs) in each hemisphere, including cortical gray matter (GM) and a layer of about 2 voxels of underlying white matter (WM). The ROIs were defined in MNI-space using the FSL Harvard–Oxford (H–O) cortical structures atlas. This atlas provides probability maps for each cortical or subcortical structure in which each voxel has an absolute value that ranges from 0 to 100, representing the percentage of subjects that have that voxel in common for that region within the atlas.

The 9 ROIs defined in each hemisphere were as follows: (1) anterior temporal lobe (ATL, used as the seed ROI), (2) occipital pole (OP), (3) pars triangularis and pars opercularis of the inferior frontal gyrus (IFG), (4) orbitofrontal cortex (OFC), (5) angular gyrus and the posterior division of supramarginal gyrus (AG/SMG), (6) temporo-occipital fusiform gyrus (Fus), and the posterior and temporo-occipital divisions of (7) the inferior temporal gyrus (ITG), (8) middle temporal gyrus (MTG), and (9) superior temporal gyrus (STG) (latter 3 regions were anteriorly delimited by the MNI coordinate $y = 96$ so as not to overlap with the ATL ROIs). These are shown schematically in Figure 1 (only for the left hemisphere).

The same analysis was then performed independently for the two hemispheres. For all the 8 ROIs used as targets in the tracking (i.e., all but the ATL), a low threshold of 30 was applied to the structures of the atlas [Behrens et al., 2007; Galantucci et al., 2011]. This means that each voxel included was represented in at least 30% of the subjects from which the atlas was obtained. This threshold value was chosen to achieve a good overlap of the ROIs with the anatomical regions in the template, while minimizing overlap between adjacent areas that could bias the results of tractography.

The ATL ROI, which was used as a seed for parcellation and tracking, was obtained by merging the temporal pole region of the H–O atlas with the anterior sections of the inferior, middle, superior, and fusiform temporal gyri, using a low threshold of 10.

The posterior extent of the ATL ROIs was not formally defined according to anatomical landmarks, but was dictated by the chosen threshold.

The ROIs thus defined were then transformed to the DWI native space for each subject, using the inverse of the

linear and nonlinear transformations as previously described, and finally binarized. The threshold values were chosen carefully to provide the best coverage of the ATL and the target regions, in all subjects in the group, after transformation to the native DWI spaces in which tracking was performed. Before running tractography, we verified the correct positioning of all transformed ROIs.

Fiber Tracking and Connectivity-Based Seed Classification

Using the ATL ROI as a seed and the other 8 ROIs as targets, probability levels for connectivity (hereafter called tracks) and the related connectivity-based seed classification (parcellation) of both the ATLs were computed using the probabilistic algorithm implemented in FSL (probtrackx) and based on Bayesian estimation of diffusion parameters (bedpostx). A 2 fiber model (multitensor approach) was assumed, and the method previously described by Behrens et al. was used [Behrens et al., 2003, 2007]. Fiber tracking was initiated from all individual voxels within the seed mask in the diffusion space, repeating the process to generate 5000 streamline samples, with a step length of 0.5 mm and a curvature threshold of 0.2.

Fiber tracking resulted in eight probabilistic maps for hemisphere, each representing the connections of the voxels included in the ATL seed with one of the eight ipsilateral target ROIs. Each voxel in the track maps had an intensity value that represented the number of tractography runs (streamlines) in the repeated sampling that successfully passed through that voxel and reached the target ROI. The highest possible intensity value of the resulting probabilistic maps was, then, the number of times the probabilistic tracking was repeated for each voxel of the seed ROI (5000) multiplied by the number of voxels of the starting seed. A low threshold, equal to 40% of the 95th percentile of the distribution of the intensity values in the voxels included in the tracks, was applied to the track maps [Galantucci et al., 2011]. This threshold allowed us to exclude background noise, avoiding an overly restrictive threshold in case the maximum intensity value was an outlier in the distribution.

Connectivity-based seed classification of the two anterior temporal lobe ROIs with the 8 ipsilateral targets was performed in parallel with the fiber tracking. For each individual voxel in the anterior temporal lobes, we computed the number of times the repeated sampling reached each of the 8 targets in the probabilistic tracking process. Each voxel of each ATL was then classified according to the particular target ROI with which it had the highest probability of connectivity using the FSL "find_the_biggest" command. In this way, clusters of commonly connected voxels (hereafter called segments) within the ATLs were obtained in each subject's DWI space.

Normalization of Group Results to MNI Space

After we performed fiber tracking and ATL parcellation in each native DWI space, the group results were transferred and normalized to MNI space.

Tracks obtained using the method described above were transformed into MNI space using the transformation matrices and were then binarized. In MNI space, a normalized track was defined using the voxels that belonged to a particular track in at least 15% of the subjects. This threshold was selected arbitrarily, as is common practice in tracking studies when reporting group results for general anatomical assessments. We verified that this (arbitrary) threshold produced results in line with the literature with regard to well-characterized major fiber bundles.

Several additional steps were required for normalization of the parcellation results. In the DWI native space for each subject, 8 nifti masks (one per target) per hemisphere were obtained using the FSL "proj_thresh" command. Each voxel in these 8 files had a value representing in percentage the relative number of times the repeated probabilistic tracking reached the related target (with a threshold fixed at 5% to eliminate noise). These masks were transformed to MNI space and their average value for the group was calculated. Finally, each voxel of the ATLs in MNI space was classified according to the particular ipsilateral target ROI with which it had the highest probability of relative connectivity in the group (analogous to the procedure used in the DWI space for each subject).

Nondominant Connections

To obtain further information about the connectivity of the ATLs—and specifically about connections that are not locally predominant—we performed two additional analyses.

First, we counted the number of streamlines starting from each voxel in the two ATLs and reaching the eight ipsilateral targets for each subject. Every voxel had previously been classified as "belonging" to a particular segment in the connectivity-based seed classification according to its maximum connectivity. We summed up values of streamlines with the eight target ROIs for all the voxels belonging to a segment. These values were subsequently averaged across subjects, and the relative connectivity of each segment with one out of the eight targets was calculated. In this way, it was possible to appreciate the nonpredominant connections within each segment.

Second, in the group-averaged results normalized to MNI space, the number of total streamlines starting from all the voxels of the ATLs and reaching the eight ipsilateral targets was counted. We also calculated the percentage of total connections between the two ATLs and the various targets. The number of connections of the ATLs for each subject on the left and right were statistically compared with Wilcoxon signed-rank tests.

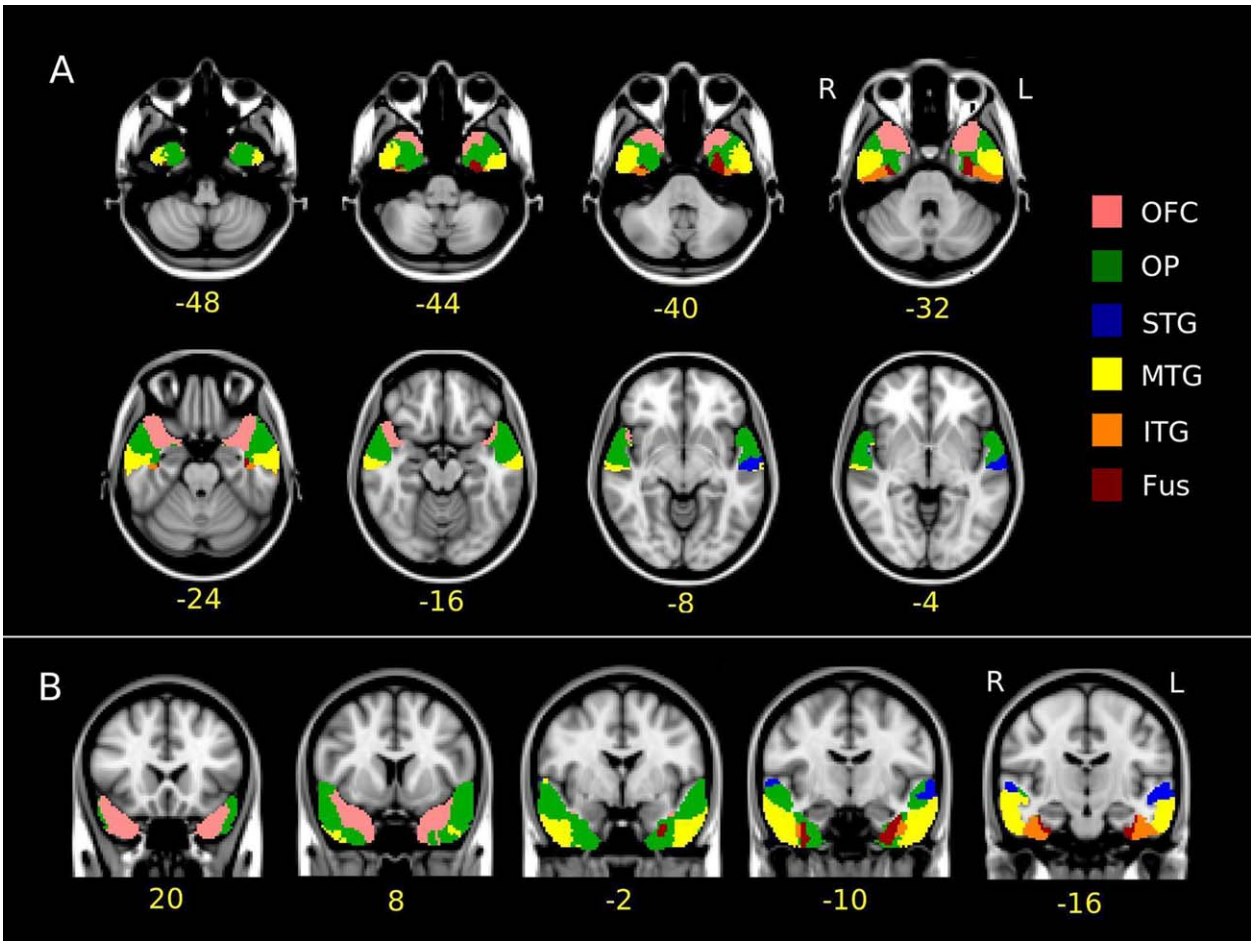

Figure 2.

(A) Axial and (B) coronal views of the parcellation result of the left and right anterior temporal lobes in the studied group normalized to the MNI space. In yellow, below the slices, the (A, top) *z* and (B, bottom) *y* MNI coordinates are reported. Voxels are colored according to the target ROI being predominantly connected with. The color code for the target ROI (reported on the right) is the same as in Figure 1.

RESULTS

Connectivity-Based Seed Classification

The connectivity-based seed classification analysis identified the target area that was predominantly connected to each voxel of the right and left ATL seed ROIs. The ATL segments resulting from this classification were visually inspected in the native DWI space and compared between subjects. The spatial arrangement of the resulting ATL segments and the overall pattern were very similar across subjects. Group results were normalized to MNI space as described above.

The classification analysis revealed very similar patterns in the two hemispheres, and identified two segments that were mainly connected to the orbitofrontal cortex and the occipital pole. In addition, four different clusters of voxels in the posterior part of the ATLs were identified as being connected predominantly with the Fus, ITG, MTG, and STG target ROIs, respectively. The spatial arrangement of these segments corresponded to the arrangement of the target ROIs, with the Fus segment being located most ventrally, and the STG segment being located most dorsally. This probably reflects the termination in the ATL of short and long connections between anterior and posterior sections of these gyri. Group results for the left and right hemispheres are reported in Figure 2.

No part of the ATL was found to be more connected to the IFG or AG/SMG target ROIs than to the other 6 target ROIs. However, many voxels in the STG segment showed a high connectivity with the AG/SMG target ROI. On the other hand, the IFG target ROI, even though it was very far from the ATL seed ROI, contributed to a certain degree

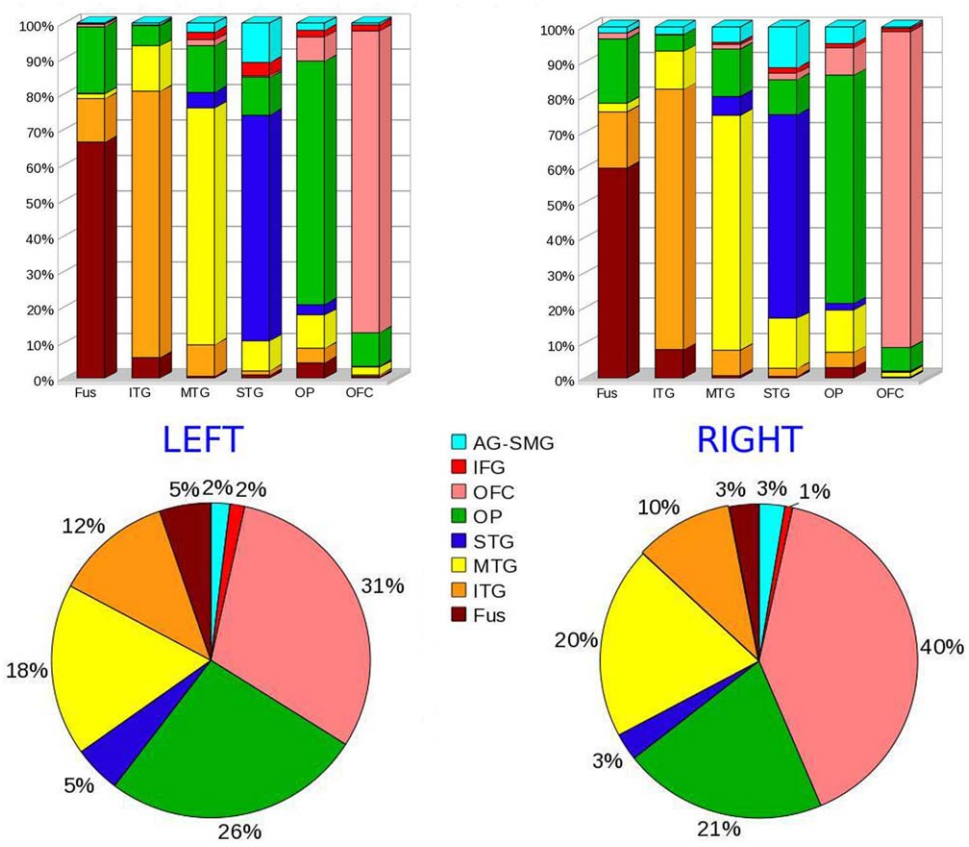

Figure 3.

Top: Bar graphs representing the relative connectivity (expressed in percentage) of each of the 6 segments resulted from the group connectivity-based seed classification (names reported under the bars) with the 8 regions used as target (names reported in the legend at the center of the figure). Bottom: Total number of connections of the ATLs with the 8 target ROIs (relative distribution). The color code in the graphs is consistent with the color of target ROIs in Figure 1.

to its overall connectivity, in particular in segments classified as being predominantly connected to the MTG and STG ROIs and, to a lesser degree, to the OP and OFC ROIs.

These findings regarding locally nondominant connections can be appreciated in histograms showing the relative connectivity between all 8 ROIs and each of the 6 segments (Fig. 3, top).

The overall relative connectivity of the two ATLs with all 8 targets is also shown in Figure 3.

As described above, the number of connections of the ATLs on the left and right for each subject was statistically compared with Wilcoxon signed-rank tests. This comparison showed that the connectivity of the ATL and OFC was higher in the right hemisphere than the left ($p = 0.0046$). On the other hand, the IFG more connected to the ATL on the left compared to the right ($p = 0.0078$).

For both the hemispheres, the strongest connections with the orbitofrontal cortex were mainly located in the medial anterior ventral temporal regions, whereas the strongest connections with the occipital pole were identified in areas more lateral and caudal.

Fiber Tracking

Probability levels for the connectivity of the left ATL with the eight target ROIs were calculated at single-subject level and normalized to MNI space as described above.

On both the left and right sides of the brain, there were strong connections between the ATL and the ipsilateral occipital pole and orbitofrontal regions through the inferior longitudinal fasciculus (ILF) and uncinate fasciculus (UF), respectively (Fig. 4 for the left hemisphere). Other pathways with high connectivity were also delineated at a group level.

The caudal/ventral part of the ATL seed (Fig. 2, orange segment) was found to be connected primarily to the superior part of the ITG target ROI, delineating a high connectivity pathway probably due to short-range white-matter fibers. In the posterior part of the ITG ROI, this pathway curves toward

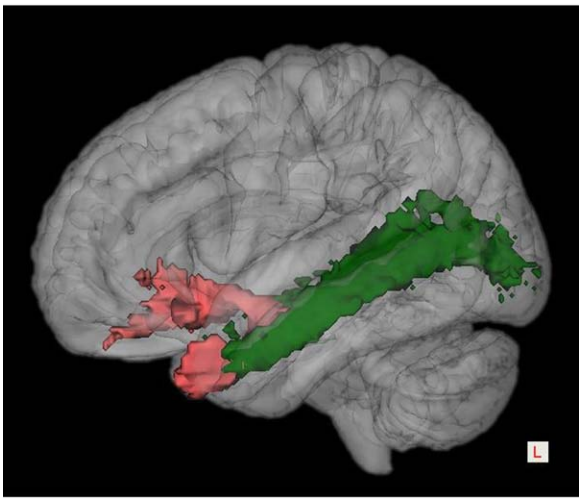

Figure 4.

3D representation of the group-averaged uncinate and the inferior longitudinal fasciculi superposed to a 3D brain rendering in the MNI space in the left hemisphere. Voxels that were visited by the fiber tracking in at least 15% of subjects are shown. The color of tracks is consistent with the target ROIs in Figure 1.

parietal and then frontal regions. Superposition across subjects is initially high, but decreases rapidly along the pathway.

Moving more medially, we found a pathway connecting the ATL (Fig. 3, dark red segment) with the posterior fusiform ROI, running parallel to the ATL-occipital pole ILF pathway. This was found consistently across subjects in both hemispheres.

Finally, we reconstructed connections between the ATL and the SMG/AG and IFG regions (Fig. 5). As discussed above and shown in Figure 3, these connections contributed modestly to the overall connectivity of the ATL, even though they were not predominant in any individual ATL segment.

DISCUSSION

Using diffusion MRI and a multitensor probabilistic fiber-tracking algorithm, we performed a structural connectivity investigation of the left and right ATLs. A set of target regions for analysis was selected on the basis of neuropsychological and neuroimaging studies suggesting the differential involvement of regions within the ATLs in networks participating in conceptual-semantic, lexical, and emotional processing. Based on the predominant connections with these regions, we were able to parcellate the ATLs into six subregions and to reconstruct the pathways that connect the ATLs with the target regions. However, we did not assume that the functional roles of these ATL subregions are defined categorically by their strongest connections; we also explored locally nondominant connections, in line with the hypothesis that multiple modality-specific connections converge in different regions of the ATLs with graded strength [Rice et al., 2015a,b].

Connections With Occipital Pole

We found strong connectivity between the ATL and the occipital pole through a pathway identifiable as the

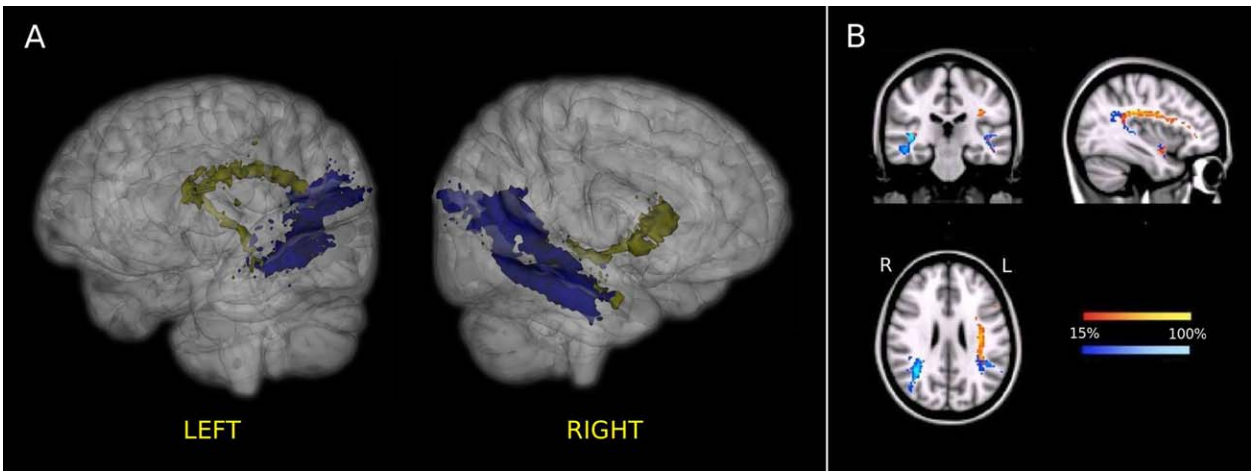

Figure 5.

Group-averaged connections of the left and right ATLs with the IFG (yellow) and the SMG/AG (blue) regions in the standard MNI space. (A) 3D representation. Voxels that were visited by the fiber tracking in at least 15% of subjects are shown. (B) 2D representation of the probability maps for the same connections. Only voxels that were visited by the fiber tracking in at least 15% of subjects of the studied group were included in the probability maps. The color scale indicates the degree of overlap among subjects.

inferior longitudinal fasciculus (ILF). The ILF was described initially in 1822 by Burdach [Polyak, 1957], and later by Dejerine [Dejerine, 1895]. It connects the occipital lobe with the anterior part of the temporal lobe, running laterally and inferiorly to the lateral wall of the temporal horn. Given the known hierarchical organization of the ventral visual pathway [Felleman and Van Essen, 1991], the robust connectivity of visual areas to the ATL through the ILF supports the general idea that the ATL is a terminus for the processing of primary sensory information.

Connections With Orbitofrontal Cortex

Overall, the greatest degree of connectivity was observed between the rostral ventro-medial portion of the ATLs and the orbitofrontal cortex bilaterally through pathways identifiable as the left and right UF [Horel and Misantone, 1976]. However, the connectivity with OFC was significantly stronger on the right hemisphere compared to the left, as quantified by the relative (Fig. 3, bottom) and absolute number of connections between the ATL and the ipsilateral OFC.

In the literature, findings of hemispheric differences in the UF are discordant. Using DTI methods, some authors have reported a leftward asymmetry in volume and fractional anisotropy values of the UF [Kubicki et al., 2002; Hasan et al., 2009], whereas other studies have reported a rightward bias. For example, in a postmortem study by Highley et al. [2002], the UF was found to be asymmetrical in both sexes, being 27% larger and containing 33% more fibers in the right than the left hemisphere [Highley et al., 2002].

The orbitofrontal cortex and UF are known to be important structures for empathic reasoning and emotional processing [Oishi et al., 2015; Rolls and Grabenhorst, 2008; Von Der Heide et al., 2013]. The finding that the OFC is strongly linked to the ATL through the UF is therefore consistent with the observation that atrophy in the anterior temporal lobes, and specifically the right anterior temporal lobe, predicts scores on measures of empathic behavior [Rankin et al., 2006].

It should be noted that the portions of the ATL that display highest connectivity to the OFC are also those that have been implicated in processing knowledge about specific persons [Damasio et al., 1996; Tranel et al., 1997] or living things [Anzellotti et al., 2011; Brambati et al., 2006; Noppeney et al., 2007]. To some extent, this may reflect the rostral convergence of information from caudally adjacent portions of the ATL [Binney et al., 2012], which in turn have connections from more distal posterior areas involved in representation of living things, such as the fusiform [Chao et al., 1999; Martin and Chao, 2001]. This might be consistent with proposals that the apparent "specificity" of the rostral ventro-medial ATL for living things may simply be a byproduct of the importance of fine-grained sensory information for distinguishing members of this category [Farah and McClelland, 1991], or the fact that living things are characterized by many shared and highly intercorrelated visual features [McRae et al., 1997; Randall et al., 2004; Rogers et al., 2004; Tyler et al., 2004].

In this light, it is tempting to speculate that the right OFC, ATL, and more posterior regions (such as fusiform gyrus) may represent nodes in a distributed network more generally involved in processing information about intentional beings. After all, empathy is predicated on the ability to pick out entities in the world with subjective experiences similar to our own—i.e., living things (as opposed to inanimate objects), and particularly conspecifics. Indeed, functional MRI studies show that judgments about social behaviors elicit activation in the superior anterior temporal cortex [Zahn et al., 2007]. It is also worth noting in this context that face perception relies on a highly right-lateralized network involving the fusiform gyrus and other temporal and occipital areas [Rossion et al., 2003, 2012]. Thus, a right-lateralized network containing information about conspecificity, emotional valence, and intentionality may support the representation of social concepts within the ATL (see also [Binney et al., 2012; Rice et al., 2015b]).

To be sure, the specialization of the right ATL for social information is almost certainly relative, and not categorical. We did find substantial connectivity between the OFC and the ATL on the left, in line with evidence that the left ATL is also engaged in processing of social concepts [Pobric et al., 2016].

Connections With Posterior Temporal Lobe

Different regions within the ATLs were strongly connected to the rostral parts of the superior temporal, middle temporal, and inferior temporal gyrus, as well as to the fusiform gyrus, in agreement with previous neuroimaging findings [Binney et al., 2012].

Connections With Perisylvian Language Regions (Angular/Supramarginal Gyrus and Inferior Frontal Gyrus)

Besides the ILF and the UF, two of the delineated connections were considered to be of remarkable interest since they involve regions known to have key roles in language processing: a connection of the ATL with the SMG/AG and a connection between the ATL and the IFG. The first pathway supports the existence of a middle longitudinal fascicle in humans [Makris et al., 2009; Bajada et al., 2015; Caverzasi et al., 2015], whereas the connection between the ATL and the IFG is thought to be a direct or indirect prolongation of the arcuate fasciculus that, in some subjects, seems to extend very anteriorly in the temporal lobe. The fact that the connection between the ATL and the IFG was stronger on the left than on the right side of the brain,

in terms of absolute and relative number of streamlines, is also consistent with a role in language processing.

Indeed, looking at results of tracking the arcuate fasciculus using other DTI approaches, mainly based on streamline deterministic algorithms [Catani et al., 2005, 2007; Turken and Dronkers, 2011], a very high intersubject variance can be observed. The point at which the arcuate fasciculus terminates in the more rostral portion of the temporal lobe (anterior to Wernicke's area) is variable. The method we used, based on a high angular resolution diffusion imaging (HARDI) acquisition and a multitensor probabilistic tracking approach, with its ability to better discriminate fiber populations within regions of complex white matter architecture [Behrens et al., 2007], might be useful to track the arcuate fasciculus more anteriorly in both its frontal and temporal terminations, at least in some subjects.

We cannot conclude unequivocally that the arcuate fasciculus always extends to regions anterior to Wernicke's area, but a certain degree of connectivity between the ATLs and the IFG was always observed. The reproducibility of this reconstructed pathway across subjects, and its relative contribution to the overall ATL connectivity, might appear to be relatively low. We think this can be explained by the potential variability among subjects of the anterior terminations of the arcuate fasciculus in the ATL, and also by the fact we used a very restrictive threshold at a subject level before transforming the tracks into MNI space. In addition, the greater distance between the ATL and the IFG ROI compared to other ROIs may partly account for the decreased superposition of results across subjects.

Connectivity of the ATL and the IFG through a "ventral pathway" was also observed for more than 33% of subjects (Fig. 5) [Ueno et al., 2011; Weiller et al., 2009]. Interestingly, this was the only ATL to IFG connection that survived for a discrete number of subjects in the right hemisphere. This pathway might represent the extreme capsule/external capsule fiber system (ECFS) [Anwander et al., 2007; Croxson et al., 2005; Frey et al., 2008; Parker et al., 2005] or part of the inferior fronto-occipital fasciculus (IFOF) [Duffau et al., 2013]. Alternatively, it could simply represent a "tracking artifact." This ventral pathway did not directly reach the triangular part of the IFG ROI, but, instead, it passed through the upper orbital part of the OFC ROI, running just above the UF. Therefore, this connection might be apparent in a few subjects within the multitensor reconstruction framework because some of the 5000 samples of connectivity drawn from each seed voxel might have taken the UF or the IFOF en route to the frontal cortex. In any case, the interpretation of this ventral pathway does not affect the parcellation result since, as described above, when group results were normalized to MNI space, no part of the ATL was found to be more connected to the IFG or AG/SMG ROIs than to the other six target ROIs.

In summary, although the ATL-IFG pathway contributes to a relatively small degree to the overall pattern of ATL connectivity shown here, this result adds to our knowledge about structural connections within the language network and is broadly in line with previous findings [Catani et al., 2005, 2007].

LIMITATIONS

One important limitation of this study is the fact that we chose to study patterns of connectivity in the ATLs using a set of ROIs defined *a priori*. Although this decision was motivated by hypotheses about the relationship of the ATLs to other regions involved in particular cognitive processes, as well as considerations of feasibility, the limitation in the number of target ROIs obviously precluded an exhaustive exploration of anterior temporal lobe connectivity.

Moreover, we used relatively large ROIs that were defined from an atlas and were not limited to gray matter (from which tracking is very difficult or impossible). This minimized *a priori* assumptions about the precise path of possible connections, gaining generality at the group-averaged level at the cost of a loss of specificity at the single-subject level. With this study, we aimed to sketch the basic framework of structural connectivity between the left and right anterior temporal lobes and other regions of the brain at a group level, without the goal of characterizing the morphology of pathways in an anatomically precise fashion on a subject-by-subject basis.

Due to time constraints in scan acquisition, we did not use an advanced acquisition method to address susceptibility distortions—such as, for example, the one used in the diffusion study by Binney et al. [Embleton et al., 2010]. Because the phase encoding direction was anterior–posterior, regions strongly affected by such distortions and in particular by a "stretching of the parenchyma" (identified to be around MNI coordinate $z = -26/-24$) were posterior and outside the ATL ROIs; therefore, most voxels in the relatively big seed ROIs in this study were not strongly affected. Moreover, the distortions affected the two hemispheres in a similar fashion, and thus would not be expected to affect the finding of interhemispheric differences. We therefore believe that our general conclusions are robust and reliable despite the decision not to use a more advanced (but time-intensive) method to address susceptibility distortions. However, it would be reasonable to verify this methodological assumption in future work.

A probabilistic tracking algorithm was also chosen with the goal of maximizing sensitivity for detecting likely connections between the ATLs and other brain regions. Deterministic tracking algorithms and diffusion models beyond DTI might provide additional anatomical specificity, but could be less sensitive, and would thus be complementary to this work.

In this context, it is important to stress the difference between measuring anatomical connections directly and using diffusion tractography to infer the presence of white matter connections between two regions and to define their strength in terms of number of streamlines. Indeed, distance

effects and complex architectures in a voxel (due to kissing, fanning, and crossing of fibers) affect the false positives and negatives. Diffusion MRI is thought to be quite reliable in delineating the stem portion of large white matter bundles, but cannot always determine the exact cortical origin and termination of fibers, particularly in regions where the white matter architecture is very complex. Determining whether the delineated pathways were direct or indirect, and exactly which cortical structures they might correspond to, was beyond the methodological scope of this study.

CONCLUSION

In this article, we presented results from a diffusion MRI study that suggest a possible functional segregation of cognitive functions within the anterior temporal lobes both within and across hemispheres, based on anatomically specific patterns of connectivity with brain regions outside the anterior temporal lobes. While the results are congruent with the idea that the anterior temporal lobes act as a representational hub for different streams of modality-specific information, they also suggest a possible anatomical basis for observed effects of regional and hemispheric specificity in processing different types of conceptual, emotional, and lexical information. Overall, our findings are broadly consistent with the hypothesis that the representation of conceptual knowledge is supported by graded connections between the anterior temporal lobes and more modality-specific cortical regions [Rice et al., 2015a,b].

ACKNOWLEDGMENTS

The study was supported by grants from the National Institutes of Health (NINDS R01 NS050915, NIA P50 AG03006, NIA P50 AG023501, NIA P01 AG019724), State of California (DHS04-35516), Alzheimer's Disease Research Centre of California (03-75271 DHS/ADP/ARCC), Larry L. Hillblom Foundation, John Douglas French Alzheimer's Foundation, Koret Family Foundation, Consortium for Frontotemporal Dementia Research, and McBean Family Foundation.

REFERENCES

Anwander A, Tittgemeyer M, von Cramon DY, Friederici AD, Knosche TR (2007): Connectivity-based parcellation of Broca's area. Cereb Cortex 17:816–825.

Anzellotti S, Mahon BZ, Schwarzbach J, Caramazza A (2011): Differential activity for animals and manipulable objects in the anterior temporal lobes. J Cogn Neurosci 23:2059–2067.

Bajada CJ, Lambon Ralph MA, Cloutman LL (2015): Transport for language south of the Sylvian fissure: The routes and history of the main tracts and stations in the ventral language network. Cortex 69:141–151.

Behrens TE, Berg HJ, Jbabdi S, Rushworth MF, Woolrich MW (2007): Probabilistic diffusion tractography with multiple fibre orientations: What can we gain? Neuroimage 34:144–155.

Behrens TE, Woolrich MW, Jenkinson M, Johansen-Berg H, Nunes RG, Clare S, Matthews PM, Brady JM, Smith SM (2003): Characterization and propagation of uncertainty in diffusion-weighted MR imaging. Magn Reson Med 50:1077–1088.

Bi Y, Wei T, Wu C, Han Z, Jiang T, Caramazza A (2011): The role of the left anterior temporal lobe in language processing revisited: Evidence from an individual with ATL resection. Cortex 47:575–587.

Binder JR, Desai RH, Graves WW, Conant LL (2009): Where is the semantic system? A critical review and meta-analysis of 120 functional neuroimaging studies. Cereb Cortex 19:2767–2796.

Binney RJ, Parker GJ, Lambon Ralph MA (2012): Convergent connectivity and graded specialization in the rostral human temporal lobe as revealed by diffusion-weighted imaging probabilistic tractography. J Cogn Neurosci 24:1998–2014.

Blaizot X, Mansilla F, Insausti AM, Constans JM, Salinas-Alaman A, Pro-Sistiaga P, Mohedano-Moriano A, Insausti R (2010): The human parahippocampal region: I. Temporal pole cytoarchitectonic and MRI correlation. Cereb Cortex 20:2198–2212.

Bozeat S, Lambon Ralph MA, Patterson K, Garrard P, Hodges JR (2000): Non-verbal semantic impairment in semantic dementia. Neuropsychologia 38:1207–1215.

Brambati SM, Myers D, Wilson A, Rankin KP, Allison SC, Rosen HJ, Miller BL, Gorno-Tempini ML (2006): The anatomy of category-specific object naming in neurodegenerative diseases. J Cogn Neurosci 18:1644–1653.

Catani M, Allin MP, Husain M, Pugliese L, Mesulam MM, Murray RM, Jones DK (2007): Symmetries in human brain language pathways correlate with verbal recall. Proc Natl Acad Sci USA 104:17163–17168.

Catani M, Jones DK, ffytche DH (2005): Perisylvian language networks of the human brain. Ann Neurol 57:8–16.

Caverzasi E, Hervey-Jumper SL, Jordan KM, Lobach IV, Li J, Panara V, Racine CA, Sankaranarayanan V, Amirbekian B, Papinutto N, Berger MS, Henry RG (2015): Identifying preoperative language tracts and predicting postoperative functional recovery using HARDI q-ball fiber tractography in patients with gliomas. J Neurosurg 11:1–13. [Epub ahead of print]

Chao LL, Haxby JV, Martin A (1999): Attribute-based neural substrates in temporal cortex for perceiving and knowing about objects. Nat Neurosci 2:913–919.

Croxson PL, Johansen-Berg H, Behrens TE, Robson MD, Pinsk MA, Gross CG, Richter W, Richter MC, Kastner S, Rushworth MF (2005): Quantitative investigation of connections of the prefrontal cortex in the human and macaque using probabilistic diffusion tractography. J Neurosci 25:8854–8866.

Damasio H, Grabowski TJ, Tranel D, Hichwa RD, Damasio AR (1996): A neural basis for lexical retrieval. Nature 380:499–505.

Damasio H, Tranel D, Grabowski T, Adolphs R, Damasio A (2004): Neural systems behind word and concept retrieval. Cognition 92:179–229.

Dejerine J (1895): Anatomie des Centres Nerveux. Paris: Rueff et Cie.

Devlin JT, Moore CJ, Mummery CJ, Gorno-Tempini ML, Phillips JA, Noppeney U, Frackowiak RS, Friston KJ, Price CJ (2002): Anatomic constraints on cognitive theories of category specificity. Neuroimage 15:675–685.

Devlin JT, Russell RP, Davis MH, Price CJ, Wilson J, Moss HE, Matthews PM, Tyler LK (2000): Susceptibility-induced loss of signal: Comparing PET and fMRI on a semantic task. Neuroimage 11:589–600.

Ding SL, Van Hoesen GW, Cassell MD, Poremba A (2009): Parcellation of human temporal polar cortex: A combined analysis of

multiple cytoarchitectonic, chemoarchitectonic, and pathological markers. J Comp Neurol 514:595–623.
Duffau H, Herbet G, Moritz-Gasser S (2013): Toward a pluricomponent, multimodal, and dynamic organization of the ventral semantic stream in humans: Lessons from stimulation mapping in awake patients. Front Syst Neurosci 7:44.
Embleton KV, Haroon HA, Morris DM, Lambon Ralph MA, Parker GJ (2010): Distortion correction for diffusion-weighted MRI tractography and fMRI in the temporal lobes. Hum Brain Mapp 31:1570–1587.
Fan L, Wang J, Zhang Y, Han W, Yu C, Jiang T (2014): Connectivity-based parcellation of the human temporal pole using diffusion tensor imaging. Cereb Cortex 24:3365–3378.
Farah MJ, McClelland JL (1991): A computational model of semantic memory impairment: Modality specificity and emergent category specificity. J Exp Psychol Gen 120:339–357.
Felleman DJ, Van Essen DC (1991): Distributed hierarchical processing in the primate cerebral cortex. Cereb Cortex 1:1–47.
Flechsig P (1920): Anatomie des menschlichen Gehirns und Rueckenmarks auf myelogenetischer Grundlage. Leipzig. G. Thieme.
Frey S, Campbell JS, Pike GB, Petrides M (2008): Dissociating the human language pathways with high angular resolution diffusion fiber tractography. J Neurosci 28:11435–11444.
Galantucci S, Tartaglia MC, Wilson SM, Henry ML, Filippi M, Agosta F, Dronkers NF, Henry RG, Ogar JM, Miller BL, Gorno-Tempini ML (2011): White matter damage in primary progressive aphasias: A diffusion tensor tractography study. Brain 134:3011–3029.
Gorno-Tempini ML, Dronkers NF, Rankin KP, Ogar JM, Phengrasamy L, Rosen HJ, Johnson JK, Weiner MW, Miller BL (2004): Cognition and anatomy in three variants of primary progressive aphasia. Ann Neurol 55:335–346.
Guo CC, Gorno-Tempini ML, Gesierich B, Henry M, Trujillo A, Shany-Ur T, Jovicich J, Robinson SD, Kramer JH, Rankin KP, Miller BL, Seeley WW (2013): Anterior temporal lobe degeneration produces widespread network-driven dysfunction. Brain 136:2979–2991.
Hasan KM, Iftikhar A, Kamali A, Kramer LA, Ashtari M, Cirino PT, Papanicolaou AC, Fletcher JM, Ewing-Cobbs L (2009): Development and aging of the healthy human brain uncinate fasciculus across the lifespan using diffusion tensor tractography. Brain Res 1276:67–76.
Highley JR, Walker MA, Esiri MM, Crow TJ, Harrison PJ (2002): Asymmetry of the uncinate fasciculus: A post-mortem study of normal subjects and patients with schizophrenia. Cereb Cortex 12:1218–1224.
Hopf A (1954): Die Myeloarchitektonik des Isocortex temporalis beim Menschen. Journal fuer Hirnforschung 1:208–279.
Horel JA, Misantone LJ (1976): Visual discrimination impaired by cutting temporal lobe connections. Science 193:336–338.
Kellenbach ML, Hovius M, Patterson K (2005): A pet study of visual and semantic knowledge about objects. Cortex 41:121–132.
Kubicki M, Westin CF, Maier SE, Frumin M, Nestor PG, Salisbury DF, Kikinis R, Jolesz FA, McCarley RW, Shenton ME (2002): Uncinate fasciculus findings in schizophrenia: A magnetic resonance diffusion tensor imaging study. Am J Psychiatry 159:813–820.
Mahon BZ, Caramazza A (2009): Concepts and categories: A cognitive neuropsychological perspective. Annu Rev Psychol 60:27–51.
Mahon BZ, Milleville SC, Negri GA, Rumiati RI, Caramazza A, Martin A (2007): Action-related properties shape object representations in the ventral stream. Neuron 55:507–520.
Makris N, Papadimitriou GM, Kaiser JR, Sorg S, Kennedy DN, Pandya DN (2009): Delineation of the middle longitudinal fascicle in humans: A quantitative, in vivo, DT-MRI study. Cereb Cortex 19:777–785.
Martin A, Chao LL (2001): Semantic memory and the brain: Structure and processes. Curr Opin Neurobiol 11:194–201.
McRae K, de Sa VR, Seidenberg MS (1997): On the nature and scope of featural representations of word meaning. J Exp Psychol Gen 126:99–130.
Moore CJ, Price CJ (1999): A functional neuroimaging study of the variables that generate category-specific object processing differences. Brain 122:943–962.
Morán MA, Mufson EJ, Mesulam MM (1987): Neural inputs into the temporopolar cortex of the rhesus monkey. J Comp Neurol 256:88–103.
Mummery CJ, Patterson K, Hodges JR, Wise RJ (1996): Generating 'tiger' as an animal name or a word beginning with T: Differences in brain activation. Proc Biol Sci 263:989–995.
Newhart M, Ken L, Kleinman JT, Heidler-Gary J, Hillis AE (2007): Neural networks essential for naming and word comprehension. Cogn Behav Neurol 20:25–30.
Noppeney U, Patterson K, Tyler LK, Moss H, Stamatakis EA, Bright P, Mummery C, Price CJ (2007): Temporal lobe lesions and semantic impairment: A comparison of herpes simplex virus encephalitis and semantic dementia. Brain 130:1138–1147.
Oishi K, Faria AV, Hsu J, Tippett D, Mori S, Hillis AE (2015): Critical role of the right uncinate fasciculus in emotional empathy. Ann Neurol 77:68–74.
Parker GJ, Luzzi S, Alexander DC, Wheeler-Kingshott CA, Ciccarelli O, Lambon Ralph MA (2005): Lateralization of ventral and dorsal auditory-language pathways in the human brain. Neuroimage 24:656–666.
Pascual B, Masdeu JC, Hollenbeck M, Makris N, Insausti R, Ding SL, Dickerson BC (2015): Large-scale brain networks of the human left temporal pole: A functional connectivity MRI study. Cereb Cortex 25:680–702.
Patterson K, Nestor PJ, Rogers TT (2007): Where do you know what you know? The representation of semantic knowledge in the human brain. Nat Rev Neurosci 8:976–987.
Pobric G, Jefferies E, Lambon Ralph MA (2010a): Category-specific versus category-general semantic impairment induced by transcranial magnetic stimulation. Curr Biol 20:964–968.
Pobric G, Jefferies E, Lambon Ralph MA (2010b): Amodal semantic representations depend on both anterior temporal lobes: Evidence from repetitive transcranial magnetic stimulation. Neuropsychologia 48:1336–1342.
Pobric G, Lambon Ralph MA, Jefferies E (2009): The role of the anterior temporal lobes in the comprehension of concrete and abstract words: rTMS evidence. Cortex 45:1104–1110.
Pobric G, Lambon Ralph MA, Zahn R (2016): Hemispheric specialization within the superior anterior temporal cortex for social and nonsocial concepts. J Cogn Neurosci 28:351–360.
Polyak S (1957): The vertebrate visual system. Chicago: University of Chicago Press.
Randall B, Moss HE, Rodd JM, Greer M, Tyler LK (2004): Distinctiveness and correlation in conceptual structure: Behavioral and computational studies. J Exp Psychol Learn Mem Cogn 30:393–406.
Rankin KP, Gorno-Tempini ML, Allison SC, Stanley CM, Glenn S, Weiner MW, Miller BL (2006): Structural anatomy of empathy in neurodegenerative disease. Brain 129:2945–2956.

Rice GE, Hoffman P, Lambon Ralph MA (2015a): Graded specialization within and between the anterior temporal lobes. Ann N Y Acad Sci 1359:84–97.

Rice GE, Lambon Ralph MA, Hoffman P (2015b): The roles of left versus right anterior temporal lobes in conceptual knowledge: An ALE meta-analysis of 97 functional neuroimaging studies. Cereb Cortex 25:4374–4391.

Rogers TT, Lambon Ralph MA, Garrard P, Bozeat S, McClelland JL, Hodges JR, Patterson K (2004): Structure and deterioration of semantic memory: A neuropsychological and computational investigation. Psychol Rev 111:205–235.

Rolls ET, Grabenhorst F (2008): The orbitofrontal cortex and beyond: From affect to decision-making. Prog Neurobiol 86:216–244.

Rossion B, Caldara R, Seghier M, Schuller AM, Lazeyras F, Mayer E (2003): A network of occipito-temporal face-sensitive areas besides the right middle fusiform gyrus is necessary for normal face processing. Brain 126:2381–2395.

Rossion B, Hanseeuw B, Dricot L (2012): Defining face perception areas in the human brain: A large-scale factorial fMRI face localizer analysis. Brain Cogn 79:138–157.

Schwartz MF, Kimberg DY, Walker GM, Faseyitan O, Brecher A, Dell GS, Coslett HB (2009): Anterior temporal involvement in semantic word retrieval: Voxel-based lesion-symptom mapping evidence from aphasia. Brain 132:3411–3427.

Seeley WW, Bauer AM, Miller BL, Gorno-Tempini ML, Kramer JH, Weiner M, Rosen HJ (2005): The natural history of temporal variant frontotemporal dementia. Neurology 64: 1384–1390.

Smith SM, Jenkinson M, Woolrich MW, Beckmann CF, Behrens TE, Johansen-Berg H, Bannister PR, De Luca M, Drobnjak I, Flitney DE, Niazy RK, Saunders J, Vickers J, Zhang Y, De Stefano N, Brady JM, Matthews PM (2004): Advances in functional and structural MR image analysis and implementation as FSL. Neuroimage 23:S208–S219.

Thompson SA, Patterson K, Hodges JR (2003): Left/right asymmetry of atrophy in semantic dementia: Behavioral-cognitive implications. Neurology 61:1196–1203.

Tranel D, Damasio H, Damasio AR (1997): A neural basis for the retrieval of conceptual knowledge. Neuropsychologia 35:1319–1327.

Tsapkini K, Frangakis CE, Hillis AE (2011): The function of the left anterior temporal pole: Evidence from acute stroke and infarct volume. Brain 134:3094–3105.

Turken AU, Dronkers NF (2011): The neural architecture of the language comprehension network: Converging evidence from lesion and connectivity analyses. Front Syst Neurosci 5:1.

Tyler LK, Stamatakis EA, Bright P, Acres K, Abdallah S, Rodd JM, Moss HE (2004): Processing objects at different levels of specificity. J Cogn Neurosci 16:351–362.

Ueno T, Saito S, Rogers TT, Lambon Ralph MA (2011): Lichtheim 2: Synthesizing aphasia and the neural basis of language in a neurocomputational model of the dual dorsal-ventral language pathways. Neuron 72:385–396.

Visser M, Lambon Ralph MA (2011): Differential contributions of bilateral ventral anterior temporal lobe and left anterior superior temporal gyrus to semantic processes. J Cogn Neurosci 23:3121–3131.

Visser M, Jefferies E, Embleton KV, Lambon Ralph MA (2012): Both the middle temporal gyrus and the ventral anterior temporal area are crucial for multimodal semantic processing: Distortion-corrected fMRI evidence for a double gradient of information convergence in the temporal lobes. J Cogn Neurosci 24:1766–1778.

Von Der Heide RJ, Skipper LM, Klobusicky E, Olson IR (2013): Dissecting the uncinate fasciculus: Disorders, controversies and a hypothesis. Brain 136:1692–1707.

Weiller C, Musso M, Rijntjes M, Saur D (2009): Please don't underestimate the ventral pathway in language. Trends Cogn Sci 13:369–370.

Woolrich MW, Jbabdi S, Patenaude B, Chappell M, Makni S, Behrens T, Beckmann C, Jenkinson M, Smith SM (2009): Bayesian analysis of neuroimaging data in FSL. Neuroimage 45: S173–S186.

Zahn R, Moll J, Krueger F, Huey ED, Garrido G, Grafman J (2007): Social concepts are represented in the superior anterior temporal cortex. Proc Natl Acad Sci USA 104:6430–6435.